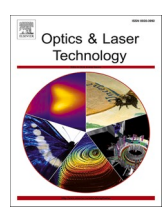
FISEVIER

Contents lists available at ScienceDirect

# Optics and Laser Technology

journal homepage: www.elsevier.com/locate/optlastec



Full length article

# Precision spectroscopy and frequency stabilization using a compact dual-mode operation cavity-enhanced absorption spectrometer at 1550 nm

Wen-Tao Wang <sup>a</sup> , Tian-Peng Hua <sup>b</sup> , Zi-Tan Zhang <sup>c</sup>, Zhi-Jian Yuan <sup>a</sup>, Yu R. Sun <sup>b</sup>, A.-W. Liu <sup>a,d,\*</sup> , S.-M. Hu <sup>a,c</sup>

- <sup>a</sup> Hefei National Laboratory, University of Science and Technology of China, Hefei 230088 Anhui, China
- <sup>b</sup> Institute of Advanced Science Facilities, ShenZhen 518107, China
- c Hefei National Laboratory for Physical Sciences at Microscale, iChem Center, University of Science and Technology of China, Hefei 230026, China
- d State Key Laboratory of Molecular Reaction Dynamics, Department of Chemical Physics, University of Science and Technology of China, Hefei 230026 Anhui, China

#### ARTICLE INFO

# Keywords: Frequency reference 1550 nm Cavity enhanced saturated absorption spectroscopy Frequency stabilization

#### ABSTRACT

The development of precision frequency references at 1550 nm is limited by scarce molecular transition options for fiber-optic communications and coherent LiDAR applications. We identify the  $3_{21}$  (101)  $\leftarrow 3_{12}$  (000) rovibrational transition of HD<sup>16</sup>O at 1549.8639 nm as a metrologically viable candidate, offering complementary capabilities to existing BIPM-recommended standards. A compact dual-mode operation cavity-enhanced absorption spectroscopy and laser stabilization via differential piezoelectric transducer (PZT) feedback for cavity length control. Using wavelength-modulated cavity-enhanced saturated absorption spectroscopy with optical frequency comb calibration, we determine the absolute transition frequency to be 193,431,476,145.8(12) kHz. The system achieves  $2 \times 10^{-12}$  frequency stability at 512 s integration time and sustains <20 kHz frequency deviation over 10-hour continuous operation with a cavity leaking rate of 0.18 Pa/hour performance rivaling conventional acetylene-based references in this spectral band. This work establishes HD<sup>16</sup>O transitions as practical frequency references for field-deployable wavelength stabilization in next-generation photonic systems operating at telecom wavelengths.

#### 1. Introduction

The rich internal degrees of freedom inherent in molecules – including vibrational modes, rotational states, and hyperfine structures – enable diverse applications through precision molecular spectroscopy [1–4]. These molecular transitions provide versatile optical frequency references spanning the entire electromagnetic spectrum while serving as critical benchmarks for frequency metrology.

Recent advances combining saturated absorption spectroscopy with optical frequency combs [5–7] have achieved unprecedented accuracy in frequency determination at the kHz level or better [8,9]. Notable implementations include He-Ne lasers stabilized to CH<sub>4</sub> transitions at 3.39  $\mu$ m [10], ND:YAG lasers stabilized to I<sub>2</sub> transitions near 1550 nm [11,12], 1064 nm [13] and 531 nm [14,15], along with near-infrared references utilizing N<sub>2</sub>O transitions at 1.28  $\mu$ m [16], H<sub>2</sub><sup>18</sup>O transition at 1.39  $\mu$ m [17], HCN and acetylene isotopologue transitions in the 1.52–1.56  $\mu$ m range [18,19,20], and CO transitions near 1.56  $\mu$ m [21].

The 1550 nm spectral region holds particular significance in modern photonics due to three key attributes: (1) compatibility with silica optical fibers' low-loss transmission window, (2) alignment with atmospheric transparency bands, and (3) operation within the eye-safe wavelength regime. Recognized by the International Telecommunication Union as a standard for dense wavelength division multiplexing, this region underpins telecommunications infrastructure [22,23]. Current molecular references in this range comprise approximately fifty  $\rm H^{13}C^{14}N$  transitions (1530—1565 nm) [18,24] and several dozen BIPM-recommended  $\rm ^{13}C_2H_2$  acetylene transitions near 1.55 µm [25]. However, practical implementation faces challenges: HCN-based systems present toxicity concerns for routine operation, while existing acetylene main isotopoluges  $\rm ^{12}C_2H_2$  references do not precisely align with the optimal 1550 nm operational wavelength.

To address these limitations, we propose an alternative frequency reference using the HD<sup>16</sup>O absorption line at 1549.89 nm. This transition offers distinct advantages: HDO samples can be safely prepared

<sup>\*</sup> Corresponding author at: Hefei National Laboratory, University of Science and Technology of China, Hefei 230088, Anhui, China. *E-mail address:* awliu@ustc.edu.cn (A.-W. Liu).

through controlled isotopic mixing of deuterated and normal water, and its line strength proves suitable for precision frequency reproduction via saturated absorption spectroscopy. In this study, we employ cavity-enhanced Lamb-dip spectroscopy for absolute frequency determination and demonstrate a compact diode laser stabilization system locked to this  $\mathrm{HD}^{16}\mathrm{O}$  transition.

#### 2. Experimental details

The experimental setup is depicted schematically in Fig. 1. The configuration was designed to implement wavelength-modulated cavity-enhanced absorption spectroscopy (1f-wm-CEAS) and to stabilize the laser frequency using an optical assembly mounted on a 30c m by 30 cm breadboard. The optical components are largely identical to those employed in our previous studies [26,27]. A custom-built tunable external cavity diode laser (ECDL), featuring a Littrow-type grating configuration [28] and utilizing the SAF1550P2 gain chip from Thorlabs Inc., operates within the wavelength range of 1530-1570 nm. This laser is split into two beams for frequency scanning and beating purposes. The scanning laser beam is phase modulated by a fiber electro-optic modulator f-EOM (EOspace, PM-0S5-20-PFA-PFA-1500/1600-UL) at a frequency of 25 MHz, and then coupled into an optical cavity. The cavity is composed of a compact 5-cm-long quartz cell housing two concave highreflectivity (HR) mirrors with a curvature radius of 1 m (Layertec GmbH Inc., R = 0.99993), yielding a free spectral range (FSR) of 2.5 GHz and a finesse of approximately 47,000. Two fast detectors are positioned before the sample cell. One servo loop maintains the f-EOM at a minimum residual amplitude modulation (RAM) signal, as monitored by an amplified InGaAs detector EOT1 (ET-3000A from Electro-Optics Technology) [29]. Another fast-detector, EOT2, monitors the back-reflected signal from the cavity, which is used to lock the laser frequency to one longitudinal mode of the cavity by the Pound-Drever-Hall (PDH) method [30] by applying a 25 MHz modulation frequency to the f-EOM. In our system, both fast and slow feedback paths are employed

simultaneously to achieve robust laser frequency lock. The fast feedback is applied to the laser current through a PID controller, while the slow feedback is sent to the piezoelectric actuator (PZT) of the laser. The optical cavity length is sinusoidally modulated at a frequency of 200 Hz by a PZT (PANT Piezo Actuators, PTH1501206101), effectively mitigating noise associated with the baseline drift. The optical cavity is enclosed within an aluminum cylinder for heat shielding and then within a temperature-stabilized stainless-steel chamber, maintaining less than 0.1 K temperature fluctuation. The transmitted laser signal is detected by a photodiode (Thorlabs, SM05PD5A) and simultaneously demodulated by a lock-in amplifier (Stanford Research Systems, SR860 500-kHz DSP Lock-in Amplifier), providing the first harmonic signal of WM-CEAS. The zero-crossing point between the Lamb-dip of molecular saturated absorption in the 1f-wm-CEAS and the baseline serves as a frequency reference for laser frequency stabilization. The beat frequency between the laser beam and an optical frequency comb (OFC) is recorded to measure the absolute laser frequency. The OFC is generated by an Er:fiber oscillator operating at a repetition rate ( $f_r \approx 8205$  MHz) and a carrier-envelope offset frequency ( $f_0 \approx 8250 \text{ MHz}$ ). Notably, it is the sum of the actual offset frequency (45 MHz) and the repetition rate that is actively stabilized. The entire system is phase-locked to a local active hydrogen maser (VCH-1003 M) serving as the frequency reference. The absolute laser frequency is expressed as:

$$\nu = f_0 + N \times f_r + f_B \tag{1}$$

where  $f_B$  denotes the beat frequency between the optical comb and the laser, and the integer N corresponds to the comb tooth index. The value of N can be determined from measurements taken with a HighFinesse wavemeter, which provides readings in THz with an accuracy of 10 MHz.

Two distinct experimental modes, "Spectral" and "Locking", are executed by applying different feedback signals to the PZT for cavity length stabilization. In the "Spectral" mode, the feedback signal is

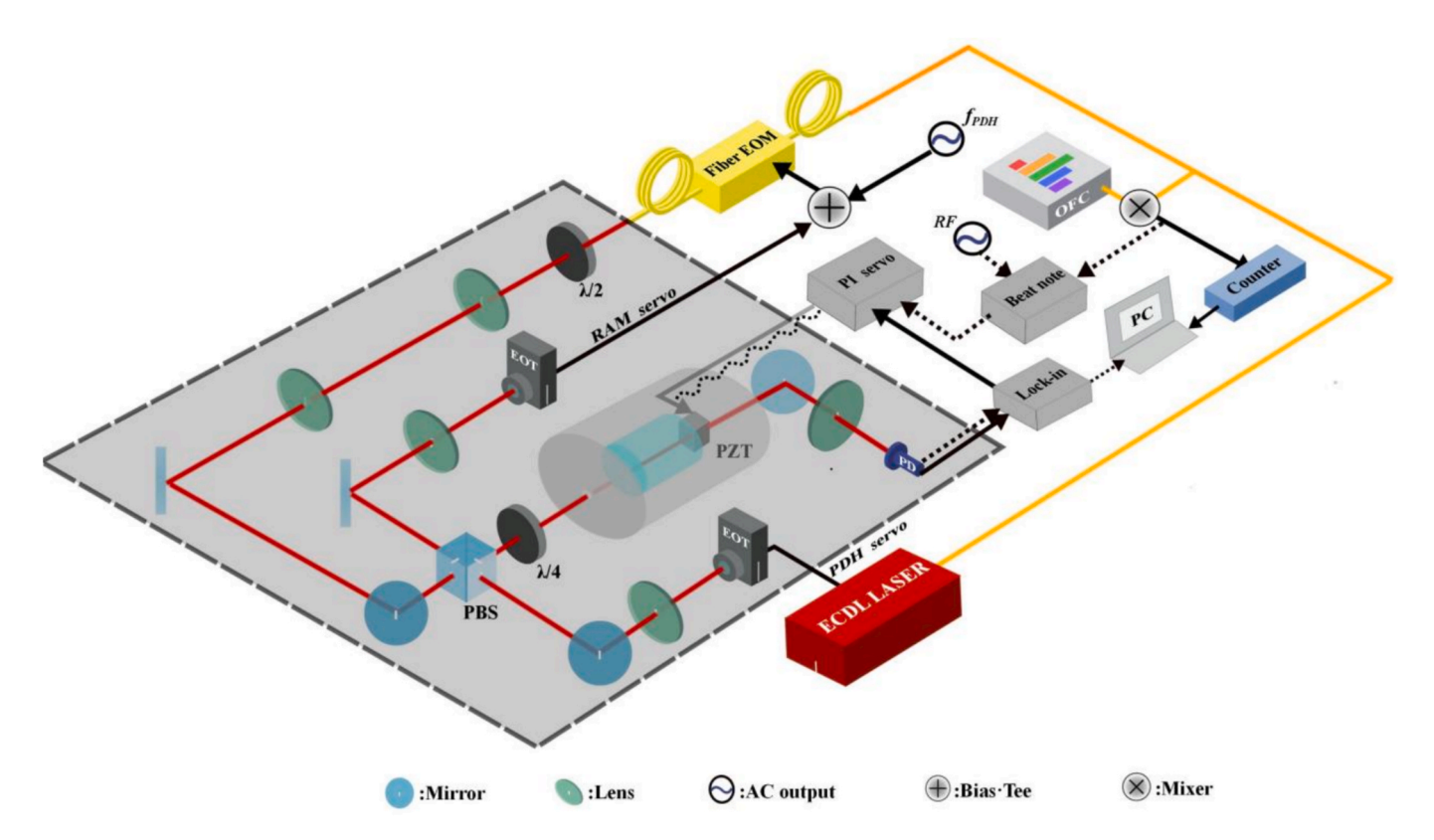


Fig. 1. Configuration of the experimental apparatus. EOT: Amplified InGaAs Detector; PBS: polarized beam splitter;  $\lambda/2$ : halfwave plate; EOM: electro-optic modulator; RAM:residual amplitude modulation; PD: photodetector.

generated by a locking servo system com- paring the beat signal to a preset radio frequency (RF) signal. By adjusting the RF frequency, we can precisely tune the laser frequency, thus implementing the "Spectral" experimental mode. Alternatively, in the "Locking" mode, the laser is continuously locked to the cavity resonance in a similar way as in the "Spectral" mode, which is achieved through a feedback signal obtained from a proportional-integral (PI) feedback servo system, utilizing the demodulated transmitted laser signal at the zero crossing point for precise control. This dual-mode approach offers flexible experimental configurations to meet specific spectroscopic or locking requirements.

Considering optical cavity leakage effects and the self pressure-shifts of  $H_2^{16}O$  transitions (in the range between -21 and +22 kHz/Pa) in the (200) [31,32] and (013) [33] vibrational bands, we systematically investigated the  $3_{21}(101) \leftarrow 3_{12}(000) \left[ J'_{K'_aK'_c}(\nu'_1\nu'_2\nu'_3) \leftarrow J''_{K''_aK''_c}(\nu''_1\nu''_2\nu''_3) \right]$ and  $4_{13}(101) \leftarrow 4_{04}(000) \text{ HD}^{16}\text{O}$  transitions near 1550 nm. These transitions exhibit relatively small air pressure-shifts under Dopplerlimited conditions [34], thereby offering strong potential for laser frequency stabilization via molecular transition-based schemes. The sample gas was prepared by introducing 10 mL of H<sub>2</sub><sup>16</sup>O and 10 mL of D<sub>2</sub><sup>16</sup>O into a dried 100 mL stainless steel container. The container was then cooled with liquid nitrogen to freeze the mixture and evacuate any residual air. After thawing to room temperature, the vaporized mixture was introduced into the optical cavity via a stainless steel tube. To ensure isotopic equilibrium on the inner walls of the cavity, the system underwent more than 20 repeated cycles of filling and evacuations. The saturated absorption spectrum was obtained under low-pressure and room-temperature conditions.

#### 3. Results and discussions

#### 3.1. Absolute line frequency determination

Fig. 2(a) presents a representative saturated 1f-wm-CEAS spectrum of the  $3_{21}(101) \leftarrow 3_{12}$  (000) transition at 1549.8639 nm, acquired through a single scan with a spectral resolution of 200 kHz across a 6 MHz range. The measurement, conducted at a sample pressure of

approximately 1.5 Pa, required an acquisition time of roughly 75 s. It can be well reproduced by the first derivation (1f) of the Lorentzian function written as follows:

$$S_{L}^{WM}(\nu) = \frac{A}{\pi} \bullet \frac{2}{\tau} \int_{0}^{\tau} \frac{\Gamma cos(2\pi f_{m}t)dt}{\left[\Delta \nu + a_{m}cos(2f_{m}t)\right]^{2} + \Gamma^{2}}$$
 (2)

where  $\Delta\nu$  corresponds to the detuning frequency from the line center  $\nu_0$ . Four parameters of the line center  $\nu_0$ , the HWHM (half width at half maximum)  $\Gamma$ , the amplitude A and the modulation amplitude  $a_m$  were determined from a non-linear fitting procedure. The modulation frequency  $f_m$ , the modulation amplitude  $a_m$  and the lock-in integral time  $\tau$  were fixed at 300 Hz, 5.0 mv and 10 ms, respectively. The spectrum was fitted according to Eq. (2) and the residuals are shown in Fig. 2(b). The SNR (signal to noise) of a single wm-CEAS spectrum is about 100.

The uncertainty budget analysis for the center frequency of the 1549.8639 nm transition is presented below, with detailed contributions from individual sources summarized in Table 1.

**Statistical:** About 700 Lamb-dip spectra of the 1549.8639 nm transition were recorded in a pressure range of 1 to 2 Pa through three independent experimental runs, with a total acquisition time of approximately 14 h. The line centers determined from all the wm-CEAS scans were collected in Fig. 2(c). The statistical uncertainty of the averaged line centers can be written as  $4.7/\sqrt{N}$  kHz, where N represents

**Table 1**Uncertainty budget for the position of the 1549.86 nm transition of HD<sup>16</sup> O isotopologue (Unit: kHz).

Source	Frequency	Uncertainty
Statistical	193 431 476 145.4	0.3
Frequency Comb		< 0.1
Cavity Locking Servo		0.4
Pressure Shift		1.0
Line profile asymmetry		0.3
Second-order Doppler	+0.42	0.01
Total	193 431 476 145.8	1.2

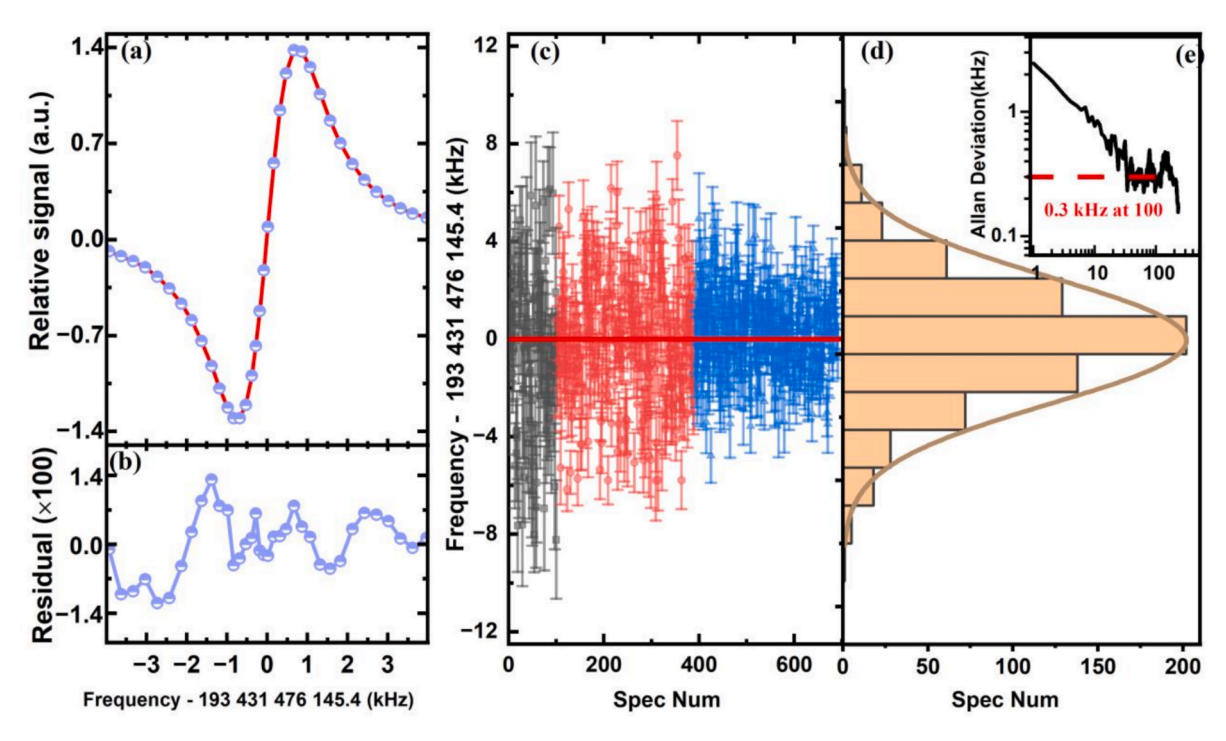


Fig. 2. (a) The saturated absorption spectrum (single scan) of the  $3_{21}$  (101)  $\leftarrow 3_{12}$  (000) transition recorded by 1f –wm-CEAS at total pressures of 1.5 Pa. (b) Fitting residuals, multiplied by a factor of 100. (c) Center frequencies obtained from about 700 scans in three experiments. (d) Histogram of the data shown in (c). The inset shows the Allan deviation of the data.

the total number of spectra used for averaging. The uncertainty decreases with  $1/\sqrt{N}$  until N  $\simeq$ 100, as shown in the Allan deviations given in the inset of Fig. 2(d). Hence, the averaged line center is 193431476.1454 MHz with a statistical uncertainty of 0.3 kHz.

**Frequency Comb:** Owing to the frequency comb being phase-locked to the hydrogen maser, we give a frequency accuracy of  $3\times 10^{-13}$ , corresponding to 0.06 kHz at 1.55  $\mu$ m. The frequency counter (BK 1823A) was also referenced to the same hydrogen maser for monitoring and reading the  $f_0$  and  $f_r$  frequency of the OFC. Therefore, the overall uncertainty of the frequency comb is less than 0.1 kHz.

**Cavity locking servo:** The frequency uncertainty due to the bias in the cavity locking servo is about 0.4 kHz estimated from the Allan deviation of the beat frequency between the laser and the frequency comb.

**Pressure Shift:** Given the leakage in the optical cavity, we systematically investigated both self and air pressure-shift effects using complementary spectroscopic techniques. The self pressure-shifts were characterized through pure water cavity ring-down spectroscopy (CRDS) measurements, utilizing the same experimental setup described in our previous work [35]. Each ring-down curve was fitted with an exponential decay function to extract the decay time  $\tau$ , and the absorption coefficient  $\alpha$  was determined from the change in the cavity loss rate according to the relation:  $\alpha = \frac{1}{c\tau} - \frac{1}{c\tau_0}$ . Simultaneously, the air pressure-shifts were precisely quantified using the current wm-CEAS system, specifically configured for air–water mixture measurements.

Fig. 3 displays the frequency centers of the saturated absorption CRDS for 1:1 mixed water samples of pure  $\rm H_2^{16}O$  and  $\rm D_2^{16}O$  across a total pressure range of 0.25 to 1.53 Pa. The self pressure-shifts  $\delta_{self}$  for the HD<sup>16</sup>O transitions at 1549.86 nm and 1551.60 nm were determined to be 1.21(29) kHz/Pa and -10.56(26) kHz/Pa, respectively, based on a linear model fit. They range from 0.025 to 0.25 times the average values reported in the work of Diouf et al. [36]. Note that the self pressure-shift effect is considered collisions between HD<sup>16</sup>O,  $\rm H_2^{16}O$  and  $\rm D_2^{16}O$  water isotopologues.

Fig. 4 illustrates the air pressure-shift  $\delta_{air}$  and pressure-broadening width  $\gamma_{air}$  effects for the HD<sup>16</sup>O transitions at 1549.86 nm and 1551.60 nm in the upper and lower panels, respectively. Notably, the wm-CEAS measurements for the air pressure effects were performed using an air–water mixture derived from a 1:1 mixture of H<sup>16</sup>O and D<sup>16</sup>O at an initial pressure of 0.3 Pa with a leakage rate of 0.18 Pa/hour. The measured air pressure-shifts for the HD<sup>16</sup>O transitions at 1549.86 nm and 1551.60 nm are 0.518(40) kHz/Pa and -5.63(24) kHz/Pa, respectively. These shifts share the same sign as the self pressure-shifts but exhibit magnitudes reduced by approximately half. In contrast,

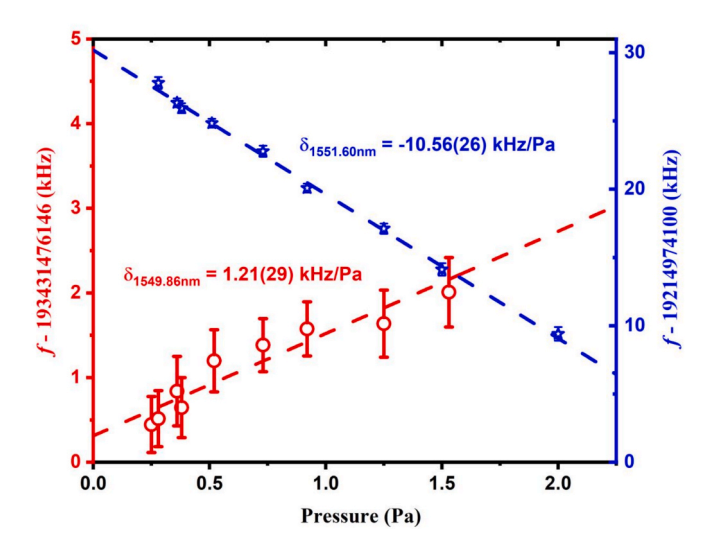


Fig. 3. Water self pressure-shifts of two different  ${\rm HD}^{16}{\rm O}$  transitions at 1549.86 nm (red circles) and 1551.60 nm (blue stars) measured with CRDS.

literature values for air pressure-shifts report -1.24 kHz/Pa and -2.36 kHz/Pa under Doppler-limited conditions for these two transitions [34], highlighting significant discrepancies. Additionally, the low-pressure air pressure-broadening width of 200 kHz/Pa exceeds the corresponding Doppler-profile values by a factor of six [34], underscoring the pronounced pressure-driven broadening effects. The frequency shifts  $f_{shift}$  to the vacuum frequency can be described with the linear relationship,  $f_{shift}$  $= \delta_{self} \times p_{water} + \delta_{air} \times p_{air}$ , where  $p_{water}$  and  $p_{air}$  denote the partial pressures (in Pa) of water vapor and air in the gas mixture, respectively. For the transitions at 1549.86 nm and 1551.60 nm, the pressure-shifts were calculated to be  $1.0\ kHz$  and  $-9.9\ kHz$  under the experimental conditions with an initial water vapor pressure of 0.3 Pa, gradually increased to a total pressure of 1.5 Pa. In analyzing the 1549.86 nm transition, we adopted a simplified approach by averaging spectral positions across the 1.0-2.0 Pa pressure range. This resulted in a self pressure shift of approximately 0.36 kHz and a maximum air pressureshift of 0.88 kHz. Therefore, we conservatively estimated the total pressure shift uncertainty to be 1.0 kHz to the overall error budget. It also indicates that the 1549.86 nm transition with smaller self and air pressure-induced shifts is a better candidate used for laser frequency

**Power shift:** The intracavity laser power is calculated to be about 4 W under 7.0 mw input excitation through combined evaluation of the vacuum cavity's transmission and the 0.15 Pa estimated partial pressure of HD<sup>16</sup>O [5,37]. The AC Stark shift is negligible at the saturation parameters S = 0.05–0.07 yielded from the saturated power  $P_s$  calculations, corresponding to pressure-broadened linewidths of 1.5–1.7 MHz (HWHM) across the 1–2 Pa gas mixture regime.

Asymmetric lineshape: In wm-CEAS, the use of a lock-in amplifier for phase- sensitive detection effectively mitigates spectral baseline fluctuations induced by laser intensity noise. Nevertheless, RAM introduced during the EOM's phase modulation process can induce spectral line shape asymmetry. This distortion manifests as systematic residual patterns exhibiting mirror asymmetry relative to the absorption line center. This effect can be quantified with an uncertainty estimation protocol based on spectral fitting residuals using the relation:  $\delta \approx \Gamma \cdot \frac{|d_{max}|}{|d_{max}|}$ , where  $d_{max}$  denotes the maximum fitting residual, and A in-

dicates the spectral peak amplitude. Through analysis of the experimental data presented in Fig. 2b, we determined a corresponding uncertainty contribution of 0.3 kHz.

**Second-order Doppler:** The second-order Doppler shift was calculated [38] based on the root-mean-square (rms) speed of HD<sup>16</sup>O molecules at room temperature (297 K). Using the kinetic theory of gases, the rms speed was determined to be 624 m/s, yielding a corresponding frequency shift of -0.42(1) kHz.

Hence, the comprehensive uncertainty is 1.2 kHz and the 1549.86 nm transition frequency is determined to be 193,431,476,145.8(12) kHz

# 3.2. Stabilized laser with HD<sup>16</sup>O transition

Using the *1f*-wm-CEAS as the error signal, the laser frequency was actively stabilized to the center of the 1549.86 nm transition via applying the feedback signal to the cavity PZT in the "Locking" mode of the experimental setup. To quantify the stabilization performance, we analyzed the heterodyne beat signal between the laser and the optical frequency comb. As shown in the upper panel of Fig. 5, the absolute frequency recorded over 10 h with a 1 Hz sampling rate reveals laser frequency fluctuations confined within a 20 kHz range around 193,431,476,145 kHz. The lower panel demonstrates that the frequency deviations follow a characteristic white noise response for integration times up to 512 s, as evidenced by the dotted-line fit showing  $\tau^{-1/2}$  dependence. Corresponding Allan deviation analysis indicates frequency stability levels of 3.0 kHz (1 s integration time) and 0.5 kHz (512 s integration time), respectively.

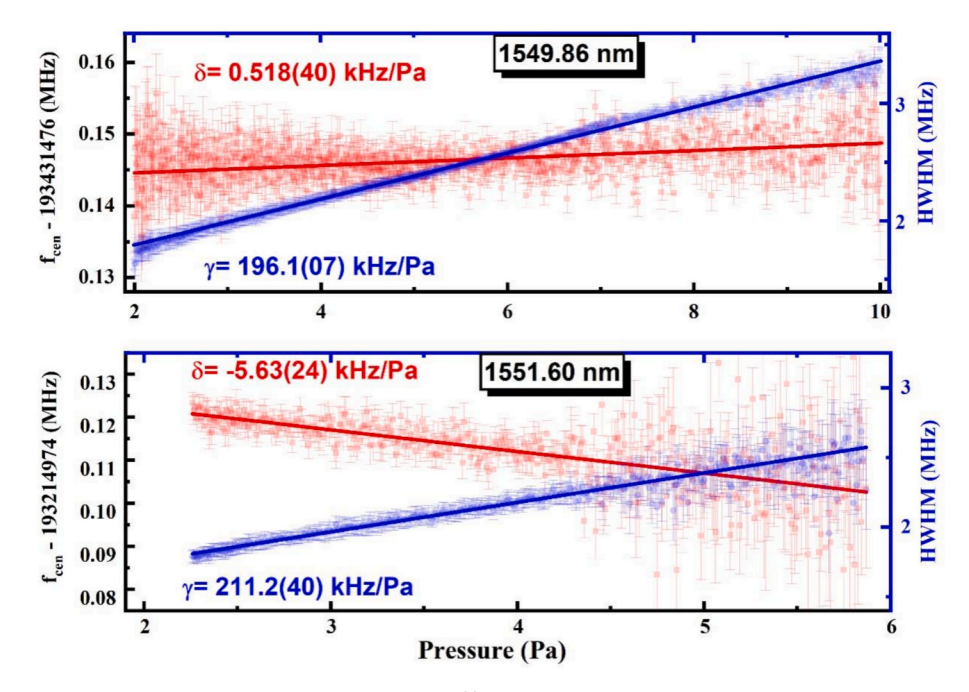


Fig. 4. Air pressure-shifts and pressure-broadening widths of two different HD<sup>16</sup>O transitions at 1549.86 nm (upper panel) and 1551.60 nm (lower panel) measured with wm-CEAS.

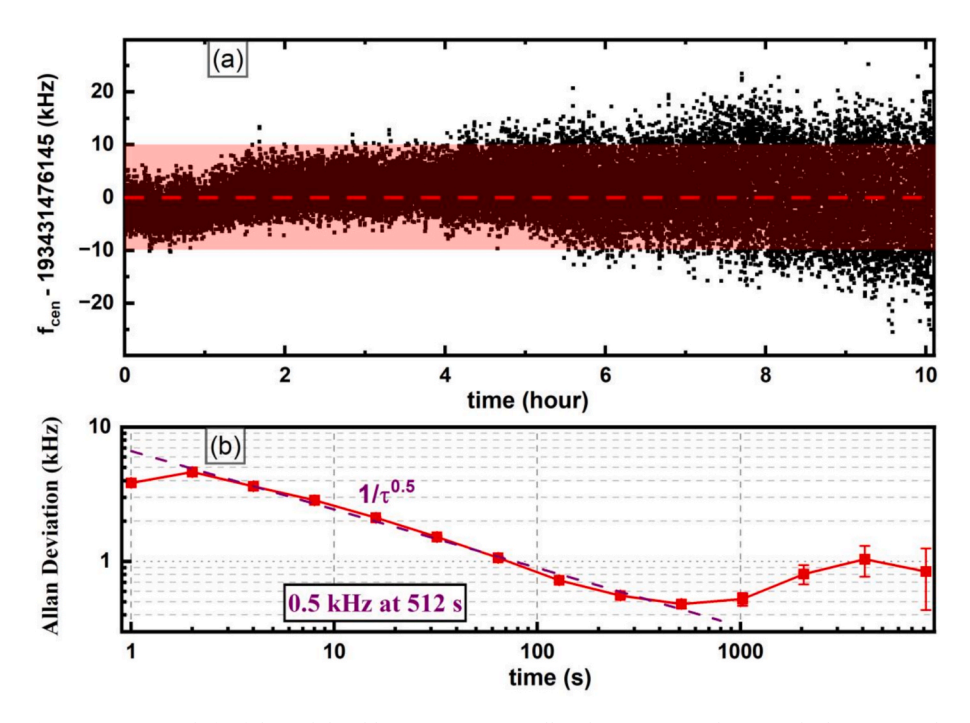


Fig. 5. Frequency drift of the stabilized-laser at 1550 nm. Allan deviations are shown in the bottom panel.

Notably, molecular line-locking experiments reveal progressive degradation of laser frequency stability approximately five hours post-lock initiation, ultimately leading to complete lock failure. This phenomenon can be attributed to the time- dependent reduction in the slope parameter (Spectral Amplitude-to-Linewidth Ratio), which serves as the critical determinant for generating effective error signals in frequency stabilization systems. During initial operation (<5 h), adequate slope magnitude enables stable frequency locking using preconfigured PI parameters. However, gradual pressure accumulation within the optical cavity progressively diminishes this critical parameter, eventually rendering the original PI settings insufficient for maintaining lock

stability.

Two mitigation strategies warrant further investigation: 1) Gas leakage reduction to maintain optimal cavity pressure conditions, and 2) Implementation of adaptive PI control algorithms capable of dynamically compensating for time-varying slope parameter variations. Both approaches show potential for achieving extended-duration frequency stabilization in the  ${\rm HD}^{16}{\rm O}$  molecular line locking systems.

## 4. Conclusions

In this work, we demonstrate the viability of the  $3_{21}(101) \leftarrow 3_{12}$ 

(000) ro-vibrational transition of  $\mathrm{HD^{16}O}$  at 1549.86 nm as a competitive frequency reference at 1550 nm. The absolute frequency of this transition was determined as 193,431,476,145.8(12) kHz with the comblocked wavelength-modulated cavity-enhanced saturated absorption spectroscopy. Its low-pressure susceptibility to self- and air-induced shifts [1.21(29) kHz/Pa and 0.518(40) kHz/Pa, respectively] underscores it as a frequency reference for 1550 nm laser stabilization in practical environments.

By frequency-locking an ECDL laser to this transition, we developed a compact frequency-stabilized laser system. Long-term stability characterization revealed  $<\!20~\text{kHz}$  frequency drift over 10-hour observation periods, demonstrating its potential for high-precision metrological applications.

## CRediT authorship contribution statement

Wen-Tao Wang: Writing – original draft, Investigation, Formal analysis, Data curation. Tian-Peng Hua: Writing – original draft, Investigation. Zi-Tan Zhang: Investigation, Data curation. Zhi-Jian Yuan: Investigation. Yu R. Sun: Writing – review & editing, Conceptualization. A.-W. Liu: . S.-M. Hu: .

#### Declaration of competing interest

The authors declare that they have no known competing financial interests or personal relationships that could have appeared to influence the work reported in this paper.

#### Acknowledgements

This work was jointly supported by NSFC (21903080 and 21688102) and CAS (XDB21020100).

This work was supported by the National Natural Science Foundation of China (Grant Nos. 22273096, 12393825) and the Innovation Program for Quantum Science and Technology (2021ZD0303102, 2021ZD0303304, 2023ZD0301002)

## Data availability

Data will be made available on request.

#### References

- [1] L.-G. Tao, A.-W. Liu, K. Pachucki, J. Komasa, Y.R. Sun, J. Wang, S.-M. Hu, Toward a determination of the proton-electron mass ratio from the Lamb-dip measurement of HD, Phys. Rev. Lett. 120 (15) (2018) 153001.
- [2] M. Quack, J. Stohner, M. Willeke, High-resolution spectroscopic studies and theory of parity violation in chiral molecules, Annu. Rev. Phys. Chem. 59 (2008) 741–769, https://doi.org/10.1146/annurev.physchem.58.032806.104511.
- [3] A.W. Liu, X.F. Li, J. Wang, Y. Lu, C.F. Cheng, Y.R. Sun, S.M. Hu, The 4ν<sub>CH</sub> overtone of <sup>12</sup>C<sub>2</sub> H<sub>2</sub>: sub-Mhz precision spectrum reveals perturbations, J. Chem. Phys. 138 (1) (2013) 1–431.
- [4] F.M.J. Cozijn, P. Dupre, E.J. Salumbides, K.S.E. Eikema, W. Ubachs, Sub-Doppler frequency metrology in HD for tests of fundamental physics, Phys. Rev. Lett. 120 (15) (2018) 153002.
- [5] G. Giusfredi, S. Bartalini, S. Borri, P. Cancio, I. Galli, D. Mazzotti, P.D. Natale, Saturated-absorption cavity ring-down spectroscopy, Phys. Rev. Lett. 104 (11) (2010) 110801.
- [6] J. Ye, L.S. Ma, J.L. Hall, Ultrasensitive detections in atomic and molecular physics: demonstration in molecular overtone spectroscopy, J. Opt. Soc. Am. B 15 (1) (1998) 6–15.
- [7] J. Ye, H. Schnatz, L.W. Hollberg, Optical frequency combs: from frequency metrology to optical phase control, IEEE J. Sel. Top. Quant. Electron. 9 (4) (2003) 1041–1058.
- [8] S. Okubo, H. Nakayama, K. Iwakuni, H. Inaba, H. Sasada, Absolute frequency list of the ν<sub>3</sub>-band transitions of methane at a relative uncertainty level of 10-11, Opt. Expr. 19 (24) (2011) 23878–23888
- [9] J. Wang, Y.R. Sun, L.G. Tao, A.W. Liu, T.P. Hua, F. Meng, S.M. Hu, Comb-locked cavity ring-down saturation spectroscopy, Rev. Sci. Instrum. 88 (4) (2017) 150801.
- [10] S.M. Foreman, Demonstration of a HeNe/CH<sub>4</sub>-based optical molecular clock, Opt. Lett. 30 (5) (2005) 570–572.

- [11] K. Ikeda, T. Kobayashi, M. Yoshiki, D. Akamatsu, F.-L. Hong, Hyperfine structure and absolute frequency of <sup>127</sup>I<sub>2</sub> transitions at 514 nm for wavelength standards at 1542 nm, J. Opt. Soc. Am. B 39 (8) (2022) 2264–2271.
- [12] A. Nishiyama, S. Okubo, T. Kobayashi, A. Kawasaki, H. Inaba, Measurement of transition frequencies and hyperfine constants of molecular iodine at 520.2 nm, J. Opt. Soc. Am. B 41 (10) (2024) 2290–2296.
- [13] K. Doeringshoff, T. Schuldt, E.V. Kovalchuk, J. Stuehler, C. Braxmaier, A. Peters, A flight-like absolute optical frequency reference based on iodine for laser systems at 1064 nm, Appl. Phys. B 123 (6) (2017) 183.1–183.8.
- [14] J. Nomura, K. Yoshii, Y. Hisai, F.-L. Hong, Precision spectroscopy and frequency stabilization using coin-sized laser modules, J. Opt. Soc. Am. B 36 (3) (2019) 631, https://doi.org/10.1364/JOSAB.36.000631.
- [15] K. Yoshii, H. Sakagami, H. Yamamoto, S. Okubo, H. Inaba, F.-L. Hong, Highresolution spectroscopy and laser frequency stabilization using a narrow-linewidth planar-waveguide external cavity diode laser at 1063 nm, Opt. Lett. 45 (1) (2020) 129, https://doi.org/10.1364/ol.45.000129.
- [16] L. Yi-Wei, C. Tzu-Ling, Sub-doppler resolution near-infrared spectroscopy at 1.28 μm with the noise-immune cavity-enhanced optical heterodyne molecular spectroscopy method, Opt. Lett. 42 (13) (2017) 2447–2450.
- [17] H. Dinesan, E. Fasci, A. Castrillo, L. Gianfrani, Absolute frequency stabilization of an extended-cavity diode laser by means of noise-immune cavity-enhanced optical heterodyne molecular spectroscopy, Opt. Lett. 39 (7) (2014) 2198, https://doi.org/ 10.1364/ol.39.002198.
- [18] S.L. Gilbert, W.C. Swann, C.-M. Wang, Hydrogen cyanide H<sup>13</sup>C<sup>14</sup>N absorption reference for 1530 nm to 1565 nm wavelength calibration–SRM 2519a, NIST Spec. Publ. 260 (2005) 137.
- [19] M. Labachelerie, K. Nakagawa, Y. Awaji, M. Ohtsu, High-frequency-stability laser at 1.5 μm using doppler-free molecular lines, Opt. Lett. 20 (6) (1995) 572–574, https://doi.org/10.1364/OL.20.000572.
- [20] Y. Zhou, J. Liu, S. Guo, G. Zhao, W. Ma, Z. Cao, L. Dong, L. Zhang, W. Yin, Y. Wu, L. Xiao, O. Axner, S. Jia, Laser frequency stabilization based on a universal sub-Doppler NICE-OHMS instrumentation for the potential application in atmospheric lidar, Atm. Meas. Tech. 12 (3) (2019) 1807–1814, https://doi.org/10.5194/amt-12-1807-2019.
- [21] S. Saraf, P. Berceau, A. Stochino, R. Byer, J. Lipa, Molecular frequency reference at 1.56 μm using a <sup>12</sup>C<sup>16</sup>O overtone transition with the noise-immune cavityenhanced optical heterodyne molecular spectroscopy method, Opt. Lett. 41 (10) (2016) 2189.
- [22] L. Zhang, X. Li, W. Luo, J. Shi, K. Sun, M. Qiu, Z. Zheng, H. Kong, J. Zhou, C. Zhang, et al., Review of 1.55 

  µm waveband integrated external cavity tunable diode lasers, Photonics 10 (11) (2023) 1287.
- [23] S.D. Setzler, M.P. Francis, Y.E. Young, J.R. Konves, E.P. Chicklis, Resonantly pumped eyesafe erbium lasers, IEEE J. Select. Top. Quant. Electron. 11 (3) (2005) 645–657.
- [24] J. Hrabina, M. Hosek, S. Rerucha, M. Cizek, Z. Pilat, M. Zucco, J. Lazar, O. Cip, Absolute frequencies of H<sup>13</sup>C<sup>14</sup>N hydrogen cyanide transitions in the 1.5 μm region with the saturated spectroscopy and a sub-kHz scanning laser, Opt. Lett. 47 (21) (2022) 5704, https://doi.org/10.1364/ol.467633.
- [25] K. Nakagawa, M.D. Labachelerie, Y. Awaji, M. Kourogi, Accurate optical frequency atlas of 1.5 μm band of acetylene, J. Opt. Soc. Am. B 13 (12) (1996) 2708.
- [26] T.-P. Hua, Y.R. Sun, S.-M. Hu, Dispersion-like lineshape observed in cavity-enhanced saturation spectroscopy of HD at 1.4 μm, Opt. Lett. 45 (17) (2020) 4863, https://doi.org/10.1364/ol.401879.
- [27] Y. Tan, Y.R. Xu, T.P. Hua, A.W. Liu, J. Wang, Y.R. Sun, S.M. Hu, Cavity-enhanced saturated absorption spectroscopy of the (30012) (00001) band of <sup>12</sup>C<sup>16</sup>O<sub>2</sub>, J. Chem. Phys. 156 (4) (2022) 044201, https://doi.org/10.1063/5.0074713.
- [28] S. Bennetts, G.D. McDonald, K.S. Hardman, J.E. Debs, C.C. Kuhn, J.D. Close, N. P. Robins, External cavity diode lasers with 5 kHz linewidth and 200 nm tuning range at 1.55 µm and methods for linewidth measurement, Opt. Expr. 22 (9) (2014) 10642–10654.
- [29] W. Zhang, M. J. Martin, C. Benko, J. L. Hall, J. Ye, C. Hagemann, T. Legero, U. Sterr, F. Riehle, G. D. Cole, Reduction of residual amplitude modulation to  $1\times 10^{-6}$  for frequency modulation and laser stabilization, Opt. Lett. 39 (7) (2014) 1980.
- [30] R.W.P. Drever, J.L. Hall, F.V. Kowalski, J. Hough, G.M. Ford, A.J. Munley, H. Ward, Laser phase and frequency stabilization using an optical resonator, Appl. Phys. B 31 (1983) 97–105, https://doi.org/10.1007/BF00702605.
- [31] R. Tóbiás, T. Furtenbacher, I. Simkó, A.G. Császár, M.L. Diouf, F.M.J. Cozijn, J.M. A. Staa, E.J. Salumbides, W. Ubachs, Spectroscopic-network-assisted precision spectroscopy and its application to water, Nat. Commun. 11 (1) (2020) 1708, https://doi.org/10.1038/s41467-020-15430-6.
- [32] M.L. Diouf, R. Tóbiás, T.S. Schaaf, F.M. Cozijn, E.J. Salumbides, A.G. Császár, W. Ubachs, Ultraprecise relative energies in the (2 0 0) vibrational band of H<sub>2</sub><sup>16</sup>O, Mol. Phys. 120 (15–16) (2022) 13, https://doi.org/10.1080/00268976 2022 2050430
- [33] J. Chen, T. P. Hua, L. G. Tao, Y. R. Sun, A. W. Liu, S. M. Hu, Absolute frequencies of water lines near 790 nm with 10<sup>-11</sup> accuracy, J. Quant. Spectrosc. Radiat. Transfer 205 (2018) 91–95. doi:10.1016/j.jqsrt.2017.10.009.
- [34] I.E. Gordon, L.S. Rothman, R.J. Hargreaves, R. Hashemi, E.V. Karlovets, F. M. Skinner, et al., The HITRAN2020 molecular spectroscopic database, J. Quant. Spectrosc. Radiat. Transf. 277 (2022) 107949, https://doi.org/10.1016/j.iosrt.2021.107049
- [35] H. Wu, C.L. Hu, J. Wang, Y.R. Sun, Y. Tan, A.W. Liu, S.M. Hu, A well-isolated vibrational state of CO<sub>2</sub> verified by near-infrared saturated spectroscopy with kHz accuracy, Phys. Chem. Chem. Phys. 22 (5) (2020) 2841–2848, https://doi.org/ 10.1039/c9cp05121j.

- [36] M.L. Diouf, R. Tóbiás, F.M.J. Cozijn, E.J. Salumbides, C. Fábri, C. Puzzarini, A. G. Császár, W. Ubachs, Parity-pair-mixing effects in nonlinear spectroscopy of HDO. Ont. Evnr. 30 (26) (2022) 46040. https://doi.org/10.1364/oe.474525
- HDO, Opt. Expr. 30 (26) (2022) 46040, https://doi.org/10.1364/oe.474525.

  [37] L.-S. Ma, J. Ye, P. Dubé, J.L. Hall, Ultrasensitive frequency-modulation spectroscopy enhanced by a high-finesse optical cavity: theory and application to
- overtone transitions of C2 H2 and C2 HD, J. Opt. Soc. Am. B 16 (12) (1999) 2255–2268.
- [38] S.N. Bagayev, V.P. Chebotayev, A.K. Dmitriyev, A.E. Om, Y.V. Nekrasov, B. N. Skvortsov, Second-order Doppler-free spectroscopy, Appl. Phys. B 52 (1991) 63–66, https://doi.org/10.1007/BF00405688.